Published in final edited form as:
Chem Res Toxicol. 2008 May ; 21(5): . doi:10.1021/tx7004458.

Protection Against Aflatoxin B_1-induced Cytotoxicity by Expression of the Cloned Aflatoxin B_1-aldehyde Reductases Rat AKR7A1 and Human AKR7A3

Sridevi Bodreddigari[#‡], **Laundette Knight Jones**[#§], **Patricia A. Egner**[§], **John D. Groopman**[§], **Carrie Hayes Sutter**[‡], **Bill D. Roebuck**[†], **F. Peter Guengerich**[¶], **Thomas W. Kensler**[§], and **Thomas R. Sutter**[‡,*]

Department of Biology and W. Harry Feinstone Center for Genomic Research, University of Memphis, Memphis, Tennessee 38152, Department of Environmental Health Sciences, Johns Hopkins Bloomberg School of Public Health, Baltimore, Maryland 21205, Department of Pharmacology and Toxicology, Dartmouth Medical School, Hanover, New Hampshire 03755, Department of Biochemistry and Center in Molecular Toxicology, Vanderbilt School of Medicine, Nashville, Tennessee 37232

[#] These authors contributed equally to this work.

Abstract

The reduction of the aflatoxin B_1 (AFB_1) dialdehyde metabolite to its corresponding mono and dialcohols, catalyzed by aflatoxin B_1-aldehyde reductase (AFAR; rat AKR7A1 and human AKR7A3), is greatly increased in livers of rats treated with numerous chemoprotective agents. Recombinant human AKR7A3 has been shown to reduce the AFB_1 dialdehyde at rates greater than those of the rat AKR7A1. The activity of AKR7A1 or AKR7A3 may detoxify the AFB_1-dialdehyde which reacts with proteins and thereby inhibit AFB_1-induced toxicity; however, direct experimental evidence of this hypothesis was lacking. Two human B lymphoblastoid cell lines, designated pMF6/1A2/AKR7A1 and pMF6/1A2, were genetically engineered to stably express AKR7A1 and/or cytochrome P4501A2 (1A2). The pMF6/1A2/AKR7A1 cells were refractory to the cytotoxic effects of 3 ng/mL AFB_1, in comparison to pM6/1A2 cells which were more sensitive. Diminished protection occurred at higher concentrations of AFB_1 in pMF6/1A2/AKR7A1 cells suggesting that additional factors were influencing cell survival. COS-7 cells were transfected with either vector control, rat AKR7A1, or human AKR7A3, and the cells were treated with AFB_1 dialdehyde. There was a 6-fold increase in the dialdehyde LC_{50}, from 66 μM in vector-transfected cells to 400 μM in AKR7A1-transfected cells, and an 8.5-fold increase from 35 μM in vector-transfected cells to 300 μM in AKR7A3-transfected cells. In both cases, this protective effect of the AFAR enzyme was accompanied by a marked decrease in protein adducts. Fractionation of the cellular protein showed that the mitochondria/nuclei and microsomal fractions contained the highest concentration of protein adducts. The levels of human AKR7A3 and AKR7A2 were measured in 12 human liver samples. The expression of AKR7A3 was detectable in all livers and lower than those of AKR7A2 in 11 of the 12 samples. Overall, these results provide the first direct evidence of a role for rat AKR7A1 and human AKR7A3 in protection against AFB_1-induced cytotoxicity and protein adduct formation.

[*]To whom correspondence should be addressed. W. Harry Feinstone Center for Genomic Research, University of Memphis, Memphis, TN 38152. (tsutter@memphis.edu)..
[‡]University of Memphis.
[§]Johns Hopkins Bloomberg School of Public Health.
[†]Dartmouth Medical School.
[¶]Vanderbilt University.

Introduction

Aflatoxin B_1 (AFB_1)[1] is a well-known naturally-occurring, carcinogen associated with the incidence of primary hepatocellular carcinoma, one of the leading causes of cancer mortality worldwide (1). AFB_1 is not itself biologically active. In humans, the initial activation is mediated through microsomal P450, particularly P4501A2 and P4503A4 (2), to generate the DNA reactive AFB_1-8,9-*exo*-epoxide (Scheme 1), which readily forms adducts with DNA (3) or hydrolyzes with water. In addition, glutathione *S*-transferase (GST) can conjugate AFB_1-8,9-*exo*-epoxide with reduced glutathione, thus preventing the formation of DNA adducts. In rats, conjugation of AFB_1-8,9-epoxide is efficiently mediated by GSTA5 subunit but in humans hGSTA1-1 and A2-2 have much lower activity towards this epoxide (4). In addition to GSTs, other detoxification mechanisms exist that may contribute to resistance to the mycotoxin. When exposed to water, AFB_1-8,9-epoxide undergoes rapid hydrolysis, forming AFB_1 dihydrodiol. This AFB_1 dihydrodiol undergoes a base-catalyzed rearrangement to, and is in equilibrium with, AFB_1 dialdehyde (5, 6, 7).

Studies in several experimental animal models have shown that the potent biological effects of AFB_1 can be inhibited by the dietary administration of specific natural or synthetic compounds (1). Several lines of evidence indicate that the protective actions of these compounds towards AFB_1 toxicity are mediated by their ability to induce detoxication enzymes such as GSTs and aflatoxin-B_1 aldehyde reductase (AFAR) (1). AFAR, a member of the NADPH-dependent aldo-keto reductase (AKR) superfamily, was purified from rat liver and shown to catalyze the reduction of the protein reactive AFB_1-dialdehyde to AFB_1-dialcohol (8). Between 6- and 18-fold increases in the levels of AFAR protein have been observed in livers of rats following administration of ethoxyquin, dithiolethiones, and other inducers (9, 10, 11). AFAR enzymes, specifically rat AKR7A1 (11, 12, 13), human AKR7A3 (11, 13, 14), and mouse AKR7A5 (15), are known to catalyze the reduction of the reactive AFB_1-derived dialdehyde at similarly high rates of activity. However, human AKR7A2 has a very high K_m for this substrate (16) and rat AKR7A4 (17) is relatively inefficient at catalyzing this reaction.

In a study of rat AKR7A1 and human AKR7A3 enzyme kinetics, it was shown that the dialdehyde was preferentially reduced to a C-8 monoalcohol, corresponding to reduction of the C-8 carbon. Production of a C-6a monoalcohol, corresponding to reduction of the C-6a carbon of the dialdehyde, occurred at a much lower rate and the formation of the dialcohol was not rapid in these reactions (17). In a subsequent study, Guengerich and coworkers (16) clearly established a role of AFB_1 dialdehyde in the formation of protein adducts. Based on the rates determined for the various reactions, these author proposed that starting with AFB_1-8,9-epoxide, the reactivity of the dialdehyde is linear over several hours. Furthermore, the fate of the dialdehyde, other than slower rearrangement to the dihydrodiol, is reaction with proteins or reduction by AFAR (16).

As this pathway of reduction by AFAR has been implicated in the prevention of AFB_1-induced cytotoxicity (8, 12) and because rat AKR7A1 is induced by compounds such as oltipraz that have been shown to protect against the toxicity of AFB_1 in the rat (18), a better understanding of this pathway is warranted. In this report we describe studies showing that expression of AKR7A1 and AKR7A3 in mammalian cells protects those cells from AFB_1- and AFB_1 dialdehyde-mediated cytotoxicity. Furthermore, we show that treatment of these

[1]**Abbreviations:** AFB_1, Aflatoxin B_1; AFAR, aflatoxin B_1-aldehyde reductase; AKR, aldo-keto reductase; CHES, 2-(N-cyclo-hexylamino)ethanesulfonate; *E.* coli, *Escherichia coli*; ECL, enhanced chemiluminescence; FP, forward primer; GST, glutathione *S*-transferase; IPTG, isopropyl-thio-β-D-galactoside; LC_{50}, lethal concentration of 50 percent of the cells; MTT, 3-(4,5-dimethylthiazoyl-2-yl)-2,5-diphenyltetrazolium bromide; *N*-NTA, nickel-nitrilotriacetic acid; NQO, 4-nitroquinoline-1-oxide; RCP, reverse complement primer.

cells with AFB_1 dialdehyde results in a dose-dependent increase in protein adducts and that the levels of these adducts are greatly diminished by the expression of either AKR7A1 or AKR7A3. To our knowledge this is the first direct evidence for prevention of protein adducts and AFB_1 dialdehyde cytotoxicity by these AFAR enzymes in cells.

Experimental Procedures

Caution

Solid aflatoxins are hazardous, and some have been demonstrated to be human carcinogens. Extreme care must be exercised when handling aflatoxins including the use of gloves, respiratory masks, and well-ventilated fume hoods. Aflatoxin residues can be destroyed using 3% bleach (e.g., Chlorox).

Chemicals and Specific Reagents

The sources include: AFB_1, Aldrich Chemical Co. (Milwaukee, WI); [^{3}H] AFB_1, Moravek Biochemicals (Brea, CA); Hygromycin B and donor horse serum, Sigma Chemical Co., (St. Louis, MO); RPMI 1640 media and the expression vector pcDNA3, Invitrogen (Carlsbad, CA); DMEM, ATCC (Manassas, VA); Fetal bovine serum, Hyclone (Logan, Utah); penicillin and streptomycin, Mediatech (Manassas, VA); DEAE-Dextran, Pharmacia Biotech (Piscataway, NJ). AFB_1 8,9-epoxide was synthesized using dimethyldioxirane (19) and hydrolyzed to AFB_1 dihydrodiol/dialdehyde.

Cell Lines and Culture Conditions

AHH-1 TK +/− cells (20) were propagated in RPMI 1640 medium supplemented with 9 % (v/v) horse serum at 37 °C in a humidified atmosphere of 5 % CO_2; monkey kidney fibroblasts (COS-7) were cultured in DMEM supplemented with 10 % FBS, penicillin (50 U/mL) and streptomycin (50 μg/mL). The pMF6/1A2 cell line was produced through transfection of a human P4501A2 cDNA into the AHH-1 TK +/− cells as described previously (20). The pMF6/1A2/AKR7A1 cell line was produced by cloning the AKR7A1 cDNA (11) into a P4501A2-containing pMF6 vector as a separate cDNA cassette with its own HSVtk promoter and polyadenylation control sequences. The pMF6 expression vector contains the Epstein Barr virus-derived OriP sequence, which allows stable replication as extrachromosomal DNA in human B lymphoblastoid cells. The construct was introduced by electroporation into the AHH-1 TK+/− cells and clones resistant to hygromycin B were selected. Selection for extrachromosomal vectors was maintained by the addition of 100–200 μg/ml hygromycin B to the cell media. COS-7 cells were transfected with the expression vectors pcDNA3, pcDNA3/AKR7A1, and pcDNA3/AKR7A3 using DEAE dextran chloroquine method (21). Briefly, the cells were transfected at 70–80 % confluency in 60 mm plates. Five μg of cDNA (AKR7A1 or AKR7A3), 10 mg/mL DEAE dextran and 100 μM chloroquine was added to each plate along with the serum free media and incubated at 37 °C /5 % CO2. After 3 h the cells were washed with PBS twice, replaced with complete media, and left for 48 hours to express the protein of interest.

Isolation of DNA and Binding

Five replicate cell cultures containing 3×10^7 cells were exposed to 3 ng/mL [^{3}H]AFB_1 (15.8 Ci/mmol) for 28 h. Nuclei were isolated and purified by the method of Marmur (22) and DNA was then purified as previously described (23). DNA content was determined colorimetrically by a diphenylamine assay (23). DNA binding was measured by liquid scintillation.

Cell Survival and Cytotoxicity Assays

For AHH-1 cell lines, relative cell survival assays were carried out as described previously (20). Cells growing in log phase were diluted to 5×10^5 cells/mL in selection medium and exposed to AFB_1 (dissolved in DMSO, final conc. < 0.1 %) at various concentrations for 28 h. Cell survival was estimated by measuring cell growth after treatment. Cell growth was determined by counting viable cells on a hemocytometer. After cultures had resumed exponential growth, the cumulative growth of the AFB_1-treated cultures was divided by the cumulative growth of the negative control cultures to calculate the relative survival (20). For COS-7 cell cytotoxicity assays, the 48 h transfected cells were seeded in a 96-well culture plate at a cell density of 2.5×10^4 and rested overnight to allow cells to adhere. The complete media was replaced by media adjusted to pH 8.2, along with different concentrations of (0, 25, 50, 100, 200, 400 μM) diol/dialdehyde that was diluted in CHES buffer, pH 10, and treated them for 4 h. The final pH of the treatment media was determined to be pH 8.2. After 4 h, the media was replaced with 100 μl of Hanks balanced salt solution pH 7.4 and 10 μl of 3-(4, 5-dimethylthiazoyl-2-yl)-2, 5-diphenyltetrazolium bromide (MTT) solution (Sigma-Aldrich) and assayed according to the manufacturer as A_{550} nm in a microplate reader (Bio-Rad, Hercules, CA). Transfection efficiencies were corrected using the β-galactosidase expression plasmid pSV-β-Gal (Promega, Madison, WI) that was cotransfected with the plasmids into the COS-7 cells. In all cases, the differences in efficiencies were less than 10 %. The lethal concentration of 50 % of the cells (LC_{50}) was calculated by linear extrapolation.

RNA Isolation and Analysis

Total cellular RNA was isolated from AHH-1 TK+/− cells by the acid guanidinum thiocyanate-phenol-chloroform extraction method as described previously (24). Poly (A)+ RNA was isolated from AHH-1 TK+/− cells and human liver samples using the Fast Track mRNA isolation system (Invitrogen). RNA blot analysis was performed as described previously (11) using cDNA probes for human P4501A2 and AKR7A1. Human liver samples were as described (13). Reverse transcription was performed according to the instructions of the manufacturer (Perkin-Elmer, Boston, MA). The reaction consists of 1x RT buffer, 5.5 mM $MgCl_2$, 0.5 mM of each dNTPs, 0.4U/L RNase inhibitor, 1.25 U/μL MMLV reverse transcriptase and 2.5 μM oligo d(T) primer. PCR was performed on the Bio-Rad iCycler (Hercules, CA) using sequence specific Taqman probes. The AKR7A2 probe (Biosearch Technologies, Novato, CA) (AACCCTTCTAAGTCAGCTTAAGGCC) was labeled with HEX (hexachloro-flurescein CE phosphoramidite); AKR7A3 with CAL RED (sulforhodamine 101); (CCAAATACTTCCATCCCTAAGAATTTACTG), and β-actin with FAM (6-carboxyfluorescein). Oligonucleotide primers, forward primer (FP) 5'-CTACTTCCGCTAGGCCCATC-3', reverse complement primer (RCP) 5'-AAAGTGAATAGGGAGCAAGG-3' for AKR7A2; FP 5'-CTACTTCCGCTAGGCCCATC-3', RCP 5'-TTTGGTGGTGACTCTTCTATTAGG-3' for AKR7A3, were obtained from IDT (Coralville, IA). The PCR mix consisted of 2x Super mix [1.5U platinum Taq DNA polymerase, 20 mM Tris-HCl (pH 8.4), 50 mM KCl, 3 mM $MgCl_2$, 400 μM dUTP, 200 μM each dGTP, dATP, dCTP, 1U UDG] (Invitrogen), 0.8 μM FP, 0.8 μM RCP, 0.2 μM Taqman probe and 50 ng cDNA in a final volume of 50 μL. Amplification was carried out as follows: denaturation for 5 min at 95 °C, 40 cycles of 95 °C for 30 s, 53 °C for 30 s, and 72 °C for 30 s, with a final extension at 72 °C for 2 min. The gene expression was calculated with the standard curve method using β-actin as an endogenous control. Standard curves were constructed with plasmid containing the cDNA of interest. The amounts of target and endogenous reference were determined from the appropriate standard curve and normalized with β-actin. Results are expressed as means ± SD (n=3).

Immunoblot Analysis

Cytosolic samples from AHH-1 TK+/− cells were analyzed as previously described (11). The cytosolic samples were separated by denaturing 12 % SDS-PAGE and electrophorectically transferred to a nitrocellulose membrane (Hybond ECL, Amersham, Arlington Heights, IL). The transferred proteins were detected by incubation of the filter with 2.5 μg/ml rabbit anti-rat AKR7A1 IgG followed by goat anti-rabbit IgG conjugated with horse-radish peroxidase (1:30,000 v/v) (Promega, Madison, WI). Immunoreactive protein was detected by enhance chemiluminescence (ECL) (Pierce Supersignal system, Rockford, IL). Amounts of AKR7A protein were estimated using purified rat recombinant proteins (1, 2, 4, 8 ng) as standards. The density values of the ECL signals were determined using a Fujix BAS1000 Bio-imaging analyzer (Fujiphoto film Co., LTD, Stamford, CT). For the selected exposure (30 s) the linearity of the ECL signals for the standard curve correspond to an r-value of 0.98, and a limit of detection of 1 ng.

Human liver cytosolic fractions were prepared from previously described samples (13). The proteins were separated by SDS-PAGE (25). *Escherichia coli* (*E. coli*) expressed-AKR7A1 and – AKR7A3 proteins were resolved on a 12 % (w/v) polyacrylamide gel containing crosslinker, *NN'*-methylenebisacrylamide (2.6 %). To increase the separation of AKR7A2 and AKR7A3 in normal human liver samples, the polyacrylamide concentration was increased to 15 % (w/v) and the concentration of *N'N'*-methylenebisacrylamide was decreases to 0.6 % (26). Gels were electrophoretically transferred onto nitrocellulose membrane (Schleicher & Schuell, Keene, NH) using the Bio-Rad Trans-Blot Cell. Incubation with primary antibody (rabbit anti-rat AKR7A1, 0.62 μg/mL), was for 1 h at room temperature. Bound antibody was detected by incubation with horseradish peroxidase-linked secondary antibody (donkey anti rabbit IgG diluted 1:30,000) (Jackson Immunoresearch, West Grove, PA). The protein was detected by ECL (Supersignal System; Pierce, Rockford, IL). ECL signals were quantified using Scion Image Software (Scion Corporation, Frederick, MD).

Slot-Blot with Lysine Adduct Antibody

The AFB_1 lysine adduct monoclonal antibody was described previously (27). COS-7 cells, transfected with pcDNA3/AKR7A3 (human), pcDNA3/AKR7A1 (rat) and pcDNA3/control, were grown to 80–90 % confluency in 60 mm dishes. The complete medium was replaced by serum free media (pH 8.2, adjusted with 1M $NaHCO_3$) containing 0, 25, 50, and 100 μM AFB_1 diol/dialdehyde dissolved in CHES buffer (pH 10). Cultures were incubated for 4 hr and then harvested, lysed, and briefly sonicated. Whole cell lysates were centrifuged at 9,000 × g for 20 min, and the supernatants were collected. For fractionation, whole cell lysates were centrifuged at 9,000 × g for 20 min and the pellet 1 was saved. The supernatant was further centrifuged at 105,000 × g for 60 min at 4 °C and the microsomal pellet and the supernatant (cytosol) were saved. The two pellets were resuspended individually in buffer "A" containing [0.1 M Tris HCl (pH 7.4), 0.1 M KCl, 1 mM EDTA, 25 μM butylated hydroxytoluene] using a pellet pestle (Kontes, Vineland, NJ). Five μg of protein was denatured in sample buffer loaded into each well of a slot-blot apparatus (Schleicher & Schull). AFB_1-derived dialdehyde protein adducts were detected using a 1:2000 dilution of the anti-lysine adduct monoclonal antibody as the primary antibody. Bound antibody was detected by incubation with horseradish peroxidase-linked secondary antibody (goat-anti mouse IgG diluted 1:10,000 (Jackson Immunoresearch, West Grove, PA) and ECL (Supersignal System; Pierce, Rockford, IL).

Statistical Analysis

Values for DNA binding and relative cell survival presented in Table 1 were analyzed by one-way analysis of variance within samples and between samples using Microsoft® Excel

2003. Cell viablility is expressed as mean ± SE and analyzed uaing a paired t-test with equal variance.

Results

Expression of AKR7A1 and P4501A2 in AHH-1 TK+/− Cells

The constructs for expression vectors pMF6/control, pMF6/1A2 and pMF6/1A2/AKR7A1 are shown in Figure 1A. These vectors were transfected into AHH-1 TK +/− cells as described in Experimental Procedures. The expected expression patterns of P4501A2 and AKR7A1 were initially confirmed by RNA blot analysis. P4501A2 expression could be detected in both pMF6/1A2 and pMF6/1A2/AKR7A1 cells, whereas no P4501A2 expression was detected in samples from pMF6/control cells (data not shown). AKR7A1 protein expression was detected in pMF6/1A2/AKR7A1 cells, whereas no AKR7A1 expression was detected in samples from pMF6/control or pMF6/1A2 cells. A single 37 kDa immunoreactive protein band was detected in cytosolic fractions prepared from pMF6/1A2/AKR7A1 cells (Figure 1B). Based on the recombinant His_6-AKR7A1 standards, the specific content of this AKR7A protein was estimated to be 0.1 μg /mg cytosolic protein. No protein bands were detected in the pMF6/control (C) or pMF6/1A2 (1A2) cells (< 20 ng AKR7A1 protein/mg protein). Thus, these cell lines appear to provide an appropriate model for testing the protective role of AKR7A1 against AFB_1.

Binding of [^{3}H] AFB_1 to Cellular DNA

The ability of AFB_1 to covalently bind to cellular DNA is dependent on its activation to the reactive AFB_1-8,9-*exo*-epoxide by P450s (28). Since P4501A2 protein expression in the cells was too low to be accurately quantified by western immunoblot analysis or by using specific enzyme assays, a DNA binding assay was used to indirectly confirm the expression of functional P4501A2 protein through its ability to activate AFB_1 to a DNA binding species. Measurement of covalently bound AFB_1 in DNA samples revealed that both P4501A2-expressing cell lines had 200-fold higher levels of DNA adducts than pMF6/control cells (Table 1). These data indicate that P4501A2 was expressed in an enzymatically active form in both the pMF6/1A2 and pMF6/1A2/AKR7A1 cell lines. More importantly, these two cell lines exhibited comparable levels of P4501A2 activation capabilities. Therefore, small differences in levels of P4501A2 activity are unlikely to account for any differences in AFB_1 dependent cytotoxicity observed in the cell lines transfected with P4501A2 or P4501A2 and AKR7A1.

To investigate the effects AFB_1, a single experiment at a concentration of 3 ng/mL was performed with five replicate cultures of each cell line. At this concentration of AFB_1, levels of DNA adducts have been shown to increase 200-fold in lymphoblastoid cell lines expressing P4501A2 (29). In both cell lines expressing P4501A2, AFB_1 binding to cellular DNA was increased more than 200-fold relative to control cells. However, while the cell line expressing only P4501A2 (pMF6/1A2) showed a significant decrease in relative survival, the cell line expressing both P4501A2 and AKR7A1 (pMF6/1A2/AKR7A1) resulted in a relative survival that was not different from the control cell line (Table 1). When concentrations of AFB_1 were increased to 10, 30, and 100 ng/mL, the AKR7A-expressing cells exhibited a concentration-dependent decrease in the proportion of cells protected against AFB_1-induced cytotoxicity (data not shown). This observation suggests that other factors are contributing to AFB_1-mediated cytotoxicity. Therefore, in order to bypass AFB_1 dialdehyde independent effects such as DNA-adduct induced apoptosis or cytotoxicity due to the P4501A2-catalyzed product AFM_1 (30), we expressed the AFAR enzymes in COS-7 cells and evaluated the toxicity of the AFB_1 dialdehyde directly using the sensitive MTT assay.

Protective Effects against AFB_1 dialdehyde in COS-7 Cells overexpressing AKR7A1 and AKR7A3

COS-7 cells were transfected with pcDNA3 expression vector carrying rat AKR7A1 and human AKR7A3 clones. Cells were then plated in a 96-well plate and challenged with AFB_1 dihydrodiol/dialdehyde at concentrations ranging from 0–400 μM. Although AFB_1 dialdehyde is known to react efficiently with lysine at pH 7.2 (16), an earlier study determined a pK_a of 8.2 for the equilibrium of AFB_1 dihydrodiol/dialdehyde (31). Therefore, cells were treated for 4 h in medium having a final pH of 8.2. At pH 7.2, the viability of COS-7 cells was 100 %. At pH 8.2, the decrease in viability to 97 % was not statistically different from the viability observed at pH 7.2. Treatment of COS-7 cells with 100 μM of AFB_1 dihydrodiol/dialdehyde (pH 7.2) for 4 h decreased the cell viability to 33 % ($p< 0.05$ relative to untreated control pH 7.2). At pH 8.2 (100 μM dihydrodiol/dialdehyde), the cell viability was further decreased to 15 % ($p< 0.05$ relative to untreated control pH 7.2), consistent with a greater concentration of AFB_1 dialdehyde at this pH (data not shown).

In cells transfected with AKR7A1, the LC_{50} increased from 66 μM in vector-transfected control cells to 400 μM in AKR7A1-transfected cells (Figure 2A). In untreated vector-transfected or AKR7A1-transfected cells, no protein adducts were detected by slot blot analysis of the total cell lysates using detection by an anti-lysine aflatoxin adduct monoclonal antibody (Figure 2B). A linear AFB_1 dialdehyde concentration dependent increase in protein adducts was observed in the vector-transfected cell treated with 0, 25, 50, and 100 μM AFB_1 dialdehyde for 4 h. The levels of these adducts were decreased in all treated cells transfected with AKR7A1, but especially at the lowest concentration of 25 μM (Figure 2C).

In cells transfected with AKR7A3, the LC_{50} increased from 35 μM in vector-transfected control cells to 300 μM in AKR7A3-transfected cells (Figure 3A). In untreated vector-transfected or AKR7A3-transfected cells, no protein adducts were detected by slot blot analysis of the total cell lysates and detection by an anti-lysine aflatoxin adduct monoclonal antibody (Figure 3B). A linear AFB_1 dialdehyde concentration dependent increase in protein adducts was observed in the vector-transfected cells treated with 0, 25, 50, and 100 μM AFB_1 dialdehyde for 4 h. The levels of these adducts were decreased in all treated cells transfected with AKR7A3, but especially at the lowest concentration of 25 μM (Figure 3C). Fractionation of the whole cell lysates (Figure 3D) revealed greater levels (on a per mg protein basis) of protein adducts in pellet 1 (mitochondrial and nuclei containing) and pellet 2 (membrane containing), than in the supernatant (cytosolic) fraction.

RNA and protein expression of human AKR7A3 and AKR7A2 in human liver

Because human AKR7A3 and AKR7A2 share 88 % amino acid identity and because both were previously shown to be expressed in human liver (11), we chose to analyze the expression of both genes in multiple human liver samples, despite the fact that AKR7A2 has a much higher K_m for AFB_1 dialdehyde (13). The open reading frames of AKR7A2 and AKR7A3 are 990 and 993 base pairs, respectively, and the predicted proteins contain 330 and 331 amino acid residues. Because of high similarity (80 %) of the AKR7A2 and AKR7A3 cDNA sequences, we could not identify specific primers in the open reading frames that could discriminate the two genes. Therefore, we used a common forward primer and specific reverse complement primers to amplify AKR7A2 and AKR7A3. The RCPs and gene specific Taqman probes were designed to anneal to unique sequences of the 3' untranslated region. β-Actin was used as endogenous control for the RT-PCR assays (32). Optimization reactions were performed to choose appropriate annealing temperatures and primer concentrations. Both genes were significantly expressed in twelve samples analyzed;

the expression of AKR7A2 was greater than that of AKR7A3 in 11 of the 12 samples (Figure 4A).

We performed immunoblot experiments using human liver cytosolic samples and recombinant proteins expressed in *E. coli* and COS-7 cells as standards. His-6-tagged AKR7A2 and AKR7A3 proteins were expressed and purified from *E. coli*. Because of an added leader sequence in the AKR7A3 *E. coli* expression construct, this protein is visibly larger than AKR7A2 when resolved on 12 % polyacrylamide gel containing 2.6 % *N′N′*-methylenebisacrylamide. Both recombinant human proteins AKR7A2 and AKR7A3 (Figure 4B) showed equally strong cross reactivity towards the antibody, indicating that any differences noted in the liver samples would be due to differences in expression levels and not to antibody reactivity. The calculated molecular weights of the non-recombinant proteins are very close. AKR7A2 has a calculated size of 36.6 kD and a pI of 6.23, while AKR7A3 has a calculated size of 37.2 kD and pI of 6.50. These characteristics make it difficult to separate the proteins by typical 1-D gel electrophoresis. COS-7 expressed proteins were resolved on 12 % polyacrylamide gel containing 2.6 % *N′N′*-methylenebisacrylamide and the mobility of the two proteins were similar (Figure 4C, upper A2 and A3 bands). In addition, the antibody reacted with a smaller non-specific protein in the COS-7 cells (Figure 4C–4D, lower NS band). Resolution of AKR7A2 and AKR7A3 (Figure 4E) was improved by increasing the acrylamide concentration to 15 % and decreasing the crosslinker concentration to 0.6 % (26). Immunoblot analysis of cytosolic fractions prepared from samples of twelve individual human livers was performed was performed under these conditions (Figure 4E). All twelve normal human livers samples expressed both AKR7A2 and AKR7A3 proteins. The levels of AKR7A2 were greater in 11 of 12 of the samples and varied by about 10-fold (Figure 4F); the levels of AKR7A3 varied by about 30-fold. Relative levels of RNA (Figure 4A) and protein (Figure 4F) do not appear to be correlated.

Discussion

We describe the development of an AHH-1 TK+/− cell line that integrates two sequential pathways of AFB_1 metabolism (Figure 1), and provide the first direct evidence in support of a role for AKR7A1 in protection against AFB_1-induced cytotoxicity. Previous cell models for toxicological assays lacked sufficient P450 to activate xenobiotics and therefore relied on extracellular activating systems; however, this generated the reactive metabolites outside the target cell (20). Our AHH-1 cell model has the ability to simultaneously express both AFB_1 activating (P4501A2) and AFB_1 dialdehyde inactivating (AKR7A1) enzymes in one system.

The pathway modeled in our cell line involves the initial activation of AFB_1 by P4501A2. Previous studies have shown that the initial metabolites formed from this reaction are the AFB_1-8,9-*exo*-epoxide, the AFB_1-8,9-*endo*-epoxide and AFM_1 (33). While only the *exo*-epoxide contributes to DNA-adduct formation, both the *exo*- and *endo*-epoxides contribute to the formation of the dihydrodiol and dialdehyde products. Although we did not measure metabolites in this study, our data are consistent with the understanding that the DNA-binding *exo*-epoxide is formed via P4501A2, as confirmed in studies which show that DNA binding occurs in P4501A2-transfected cells at a level two logs greater than in control cells. This data also shows that P4501A2-expressing cells (with or without AKR7A1) treated with 3 ng/mL AFB_1 can activate AFB_1 to the same extent. It is not clear whether the induction of DNA-binding at this particular concentration promotes cytotoxicity in these cells; however, it is suspected that if DNA binding were the only cause of cytotoxicity, then the cytotoxic response in these two cells would be the similar. At a concentration of AFB_1 of 3ng/mL, our data do not support the hypothesis that DNA binding is cytotoxic. Rather, there is a significant increase in cytotoxicity in cells expressing P4501A2 alone compared to those

coexpressing both P4501A2 and AKR7A1. This observation indicates a specific role for AKR7A1 in protection against AFB_1, promoting survival of cells exposed to this concentration of carcinogen.

The proportion of AFB_1-epoxide formed that does not bind to DNA is expected to either undergo conjugation with GSH to form the AFB_1-SG conjugate through the actions of the GST family of enzymes, or to undergo rapid, nonenzymatic hydrolysis to form AFB_1 dihydrodiol (33). Although we did not measure the expression of GSTs in this particular study, previous studies have demonstrated that the level of GSTs in these cells are negligible (20). In the case of AFB_1 dihydrodiol, this metabolite can undergo a slow, base-catalyzed ring opening to a dialdehyde (7, 31) that is capable of forming Schiff base adducts with protein amino groups, particularly lysine (16). Previous studies suggest that this type of reaction could be involved in the acute toxicity of AFB_1 (12). Based on these studies, we believe that the observed increase in survival in cells co-expressing P4501A2 and AKR7A1 is due to the ability of AKR7A1 to reduce the AFB_1-dialdehyde to non-protein binding mono- and dialcohol products.

At higher concentrations of AFB_1, the AKR7A1-expressing cells exhibited a concentration-dependent decrease in the proportion of cells protected against AFB_1-induced cytotoxicity. This observation suggests that other factors are contributing to AFB_1-mediated cytotoxicity. Of interest to this discussion, independent studies have demonstrated the apparent saturation of mutation induced by exposure to AFB_1 in human lymphoblast cell lines (29, 34). This plateau in mutant fraction is observed despite linear increases in the amount of aflatoxin-adduct formed (29, 34), and in both studies occurs at concentrations of AFB_1 exceeding 6 ng/mL. Having controlled for cell cycle and the potential for different subpopulations of cells, these studies support the concept of a disproportionate loss of cells exceeding some threshold of DNA damage. For example, apoptotic mechanisms activated at elevated levels of DNA damage could account for the concentration-dependent loss of protection afforded by AKR7A1. The similarities of the AFB_1 concentrations corresponding to these different effects make this an interesting area of future study.

As another possibility, an alternate pathway of toxicity could be mediated through AFM_1 (30). AFM_1 is formed from AFB_1 through a hydroxylation reaction catalyzed predominantly via P4501A2 (33). In previous studies, this AFM_1 metabolite retained about the same toxicity as AFB_1 for 1-day-old ducklings and rats (33). Furthermore, recent studies have reported that AFM_1 can bind to microsomal proteins, and this binding is suggested to play a role in the cytotoxicity seen in lymphoblastoid cells treated with AFB_1 (35).

As a third possibility, the lack of protection against AFB_1 cytotoxicity at higher AFB_1 concentrations could be due to an inability of the AFB_1 dialcohol metabolite to exit the cell. This metabolite might accumulate and cause feedback inhibition of further AFB_1 dialdehyde reduction or it might accumulate and cause cytotoxicity itself. Townsend and coworkers have shown that the failure of GST expression to confer resistance to 4-nitroquinoline-1-oxide (NQO) cytotoxicity is associated with transient accumulation of the NQO glutathione conjugate in MCF-7 cells expressing hGSTP1-1 (36). Yet when the multidrug resistance associated protein is expressed in MCF-7 cells, expression of transfected hGSTP1-1 does result in high level (40-fold) resistance to NQO cytotoxicity (36). However, this possibility seems unlikely, when considering the results of the AFAR-transfected COS-7 cells treated with AFB_1 dialdehyde.

COS-7 cells transfected with rat AKR7A1 showed protection against the concentration dependent increase in cytotoxicity following treatment with AFB_1 dialdehyde. This resulted in a 6-fold increase in the AFB_1 dialdehyde LC_{50}, from 66 μM in vector-transfected cells to

400 μM in AKR7A1-transfected cells. This protective effect of AKR7A1 was accompanied by a marked decrease in protein adducts. Similarly, human AKR7A3 protected cells treated with AFB_1 dialdehyde, shifting the LC_{50} 8.5-fold from 35 μM in vector-transfected cells to 300 μM in AKR7A3-transfected cells. Again this protective effect was accompanied by a marked decrease in protein adducts. Fractionation of the cellular protein showed that the mitochondria/nuclei and microsomal fractions contained the highest concentration of protein adducts. The observation of high protein adducts in the nuclear/mitochondrial fraction is of interest in regards to the report of Groopman and co-workers showing the distribution of radiolabeled AFB_1 to the nuclear fraction, its association with histone proteins, and its slower removal than for DNA adducts (37). A later study (38) showed retention of the AFB_1 histone adducts during cellular replication. As most of the protein reactivity of AFB_1 has been associated with the dialdehyde, rather than the epoxide (16), AFAR proteins could provide valuable protection against such protein adducts. While the specific cytotoxic mechanism of the dialdehyde has not been determined, binding to critical cellular proteins such as histones is a plausible contributor.

The particular events that follow enzyme induction by certain dietary compounds that result in cancer chemoprevention of AFB_1 are complex and not fully understood. The results presented here indicate that the functional significance of the elevation of AKR7A1 expression in response to certain chemoprotective agents is to inhibit AFB_1-induced cytotoxicity to cells. *In vivo*, the ability of AKR7A1 to protect against AFB_1-induced cytotoxicity could act to inhibit the compensatory hyperplasia that occurs following cell necrosis. Prevention of such compensatory hyperplasia may attenuate several steps in AFB_1 carcinogenesis including initiation, promotion and progression (39). Based on these observations, the future development of an AKR7A1 transgenic animal model to examine the role of AKR7A1 *in vivo* appears warranted. Furthermore, the expression in most human livers of the AFAR enzyme AKR7A3 indicates a need for further studies of this pathway in human AFB_1-mediated hepatocellular carcinoma.

Acknowledgments

We thank Charles Crespi, Dorothy, Crespi and Bruce Penman (BD Bioscience) for facilitating the production of the described AHH-1 TK+/− cells lines; Ying Li, Trisha Patterson, Jackie Lavigne (Johns Hopkins University), for helpful discussions. Supported by US Public Health Service grants R01 CA63922, CA39146, ES010546, and ES08148, P30 ES03819 and ES000267, and T32 ES07141.

References

(1). Kensler TW, Groopman JD, Sutter TR, Curphey TJ, Roebuck BD. Development of cancer chemopreventive agents: oltipraz as a paradigm. Chem. Res. Toxicol. 1999; 12:113–126. [PubMed: 10027787]

(2). Gallagher EP, Kunze KL, Stapleton PL, Eaton DL. The kinetics of aflatoxin B1 oxidation by human cDNA - expressed and human liver microsomal cytochromes P450 1A2 and 3A4. Toxicol. Appl. Pharmacol. 1996; 141:595–606. [PubMed: 8975785]

(3). Iyer RS, Coles FF, Raney KD, Their RP, Guengerich FP, Harris TM. DNA adduction by the potent carcinogen aflatoxin B1: mechanistic studies. J. Am. Chem. Soc. 1994; 116:1603–1609.

(4). Eaton DL, Bammler TK. Concise review of the glutathione *S*-transferases and their significance to toxicology. Toxico. Sci. 1999; 49:156–164.

(5). Patterson DS, Roberts BA. The formation of aflatoxins B2a and G2a and their degradation products during the in vitro detoxification of aflatoxin by livers of certain avian and mammalian species. Food Cosmet. Toxicol. 1970; 8:527–538. [PubMed: 5492926]

(6). Neal GE, Judah DJ, Green JA. The in vitro metabolism of aflatoxin B1 catalyzed by hepatic microsomes isolated from control or 3-methylcholanthrene-stimulated rats and quail. Toxicol Appl Pharmacol. 1986; 82:454–460. [PubMed: 3082038]

(7). Sabbioni G, Skipper PL, Buchi G, Tannenbaum SR. Isolation and characterization of the major serum albumin adduct formed by aflatoxin B1 in vivo in rats. Carcinogenesis. 1987; 8:819–824. [PubMed: 3111739]

(8). Hayes JD, Judah DJ, Neal GE. Resistance to aflatoxin B1 is associated with the expression of a novel aldo-keto reductase which has catalytic activity towards a cytotoxic aldehyde-containing metabolite of the toxin. Cancer Res. 1993; 53:3887–3894. [PubMed: 8395332]

(9). Ellis EM, Judah DJ, Neal GE, O'Connor, T. Hayes JD. Regulation of carbonyl-reducing enzymes in rat liver by chemoprotectors. Cancer Res. 1996; 56:2758–2766. [PubMed: 8665510]

(10). Anderson L, Steele VK, Kelloff GJ, Sharma S. Effects of oltipraz and related chemopreventative compounds on gene expression in rat liver. J. Cell. Biochem. 1995; 22:108–116.

(11). Knight LP, Primiano T, Groopman JD, Kensler TW, Sutter TR. cDNA cloning, expression and activity of a second human aflatoxin B_1-metabolizing member of the aldo-keto reductase superfamily, AKR7A3. Carcinogenesis. 1999; 20:1215–1223. [PubMed: 10383892]

(12). Ellis EM, Judah DJ, Neal GE, Hayes JD. An ethoxyquin-inducible aldehyde reductase from rat liver that metabolizes aflatoxin B_1 defines a subfamily of aldo-keto reductases. Proc. Natl. Acad. Sci. USA. 1993; 90:10350–10354. [PubMed: 8234296]

(13). Guengerich FP, Cai H, McMahon M, Hayes JD, Sutter TR, Groopman JD, Deng Z, Harris TM. Reduction of aflatoxin B_1 dialdehyde by rat and human aldo-keto reductases. Chem. Res. Toxicol. 2001; 14:727–737. [PubMed: 11409944]

(14). Ireland LS, Harrision DJ, Neal GE, Hayes JD. Molecular cloning, expression and catalytic activity of a human AKR7 member of the aldo-keto reductase superfamily: evidence that the major 2-carboxybenzaldehyde reductase from human liver is a homologue of rat aflatoxin B_1-aldehyde reductase. Biochem. J. 1998; 332:21–34. [PubMed: 9576847]

(15). Hinshelwood A, McGarvie G, Ellis EM. Substrate specificity of mouse aldo-keto reductase AKR7A5. Chem. Biol. Interact. 2003; 144:263–269. [PubMed: 12604212]

(16). Guengerich FP, Arneson KO, Williams KM, Deng Z, Harris TM. Reaction of aflatoxin B_1 oxidation products with lysine. Chem. Res. Toxicol. 2002; 15:780–792. [PubMed: 12067245]

(17). Kelly VP, Ireland LS, Ellis EM, Hayes JD. Purification from rat liver of a novel constitutively expressed member of the aldo-keto reductase 7 family that is widely distributed in extrahepatic tissues. Biochem. J. 2000; 348:389–400. [PubMed: 10816434]

(18). Liu YL, Roebuck BD, Yager JD, Groopman JD, Kensler TM. Protection by 5-(2-pyrazinyl)-4-methyl-1,2-dithiol-3-thione (oltipraz) against the hepatotoxicity of aflatoxin B_1 in the rat. Toxicol. Appl. Pharmacol. 1988; 93:442–451. [PubMed: 3130679]

(19). Baertschi SW, Raney KD, Stone MP, Harris TM. Preparation of the 8,9-epoxide of the mycotoxin aflatoxin B_1: the ultimate carcinogenic species. J. Am. Chem. Soc. 1988; 110:7929–7931.

(20). Crespi CL, Langenbach R, Penman BW. Human cell lines, derived from AHH-1 TK +/− human lymphoblasts, genetically engineered for expression of cytochromes P450. Toxicology. 1993; 82:89–104. [PubMed: 8236284]

(21). Luthman H, Magnusson G. High efficiency polyoma DNA transfection of chloroquine treated cells. Nucleic Acids Res. 1983; 11:1295–308. [PubMed: 6298741]

(22). Marmur JA. A procedure for the isolation of deoxyribonucleic acid from microorganisms. J. Mol. Biol. 1961; 3:208–218.

(23). Richards GM. Modifications of the diphenylamine reaction giving increased sensitivity and simplicity in the estimation of DNA. Anal. Biochem. 1974; 57:369–376. [PubMed: 4819731]

(24). Chomczynski P, Sacchi N. Single-step method of RNA isolation of acid guanidinium thiocyanate-phenol-chloroform extraction. Anal. Biochem. 1987; 162:156–159. [PubMed: 2440339]

(25). Laemmli UK. Cleavage of structural proteins during the assembly of the head of bacteriophage T4. Nature. 1970; 227:680–685. [PubMed: 5432063]

(26). Hayes JD, Mantle TJ. Use of immuno-blot techniques to discriminate between the glutathione S-transferase Yf, Yk, Ya, Yn/Yb and Yc subunits and to study their distribution in extrahepatic tissues. Evidence for three immunochemically distinct groups of transferase in the rat. Biochem. J. 1986; 233:779–788. [PubMed: 3707525]

(27). Wang JS, Abubaker S, He X, Sun G, Strickland PT, Groopman JD. Development of aflatoxin B(1)-lysine adduct monoclonal antibody for human exposure studies. Appl. Environ. Microbiol. 2001; 67:2712–2717. [PubMed: 11375185]

(28). Essigmann JM, Croy RG, Nadzan AM, Busby WF Jr. Reinhold VN, Wogan GN. Structural identification of the major DNA adduct formed by aflatoxin B_1 *in vitro*. Proc. Natl. Acad. Sci. USA. 1977; 74:1870–1874. [PubMed: 266709]

(29). Crespi CL, Steimel DT, Aoyama T, Gelboin HV, Gonzalez FJ. Stable expression of human cytochrome P4501A2 cDNA in a human lymphoblastoid cell line: Role of the enzyme in the metabolic activation of aflatoxin B_1. Mol. Carcinogenesis. 1990; 3:5–8.

(30). Roebuck, BD.; Maxuitenko, YY. Biochemical mechanisms and biological implications of the toxicity of aflatoxins as related to aflatoxin carcinogenesis. In: Eaton, DL.; Groopman, JD., editors. The Toxicology of Aflatoxins: Human Health, Verterinary, and Agricultural Significance. Academic Press; New York: 1994. p. 27-43.

(31). Johnson WW, Harris TM, Guengerich FP. Kinetics and mechanism of hydrolysis of aflatoxin B_1 *exo*-8,9-oxide and rearrangement of the dihyrodiol. J. Am. Chem. Soc. 1996; 118:8213–8220.

(32). Kreuzer KA, Lass U, Landt O, Nitsche A, Laser J, Ellerbrok H, Pauli G, Huhn D, Schmidt CA. Highly sensitive and specific fluorescence reverse transcription-PCR assay for the pseudogene-free detection of beta-actin transcripts as quantitative reference. Clin. Chem. 1999; 45:297–300. [PubMed: 9931059]

(33). Eaton, DL.; Ramsdell, HS.; Neal, GE. Biotransformation of aflatoxins. In: Eaton, DL.; Groopman, JD., editors. The Toxicology of Aflatoxins: Human Health, Verterinary, and Agricultural Significance. Academic Press; New York: 1994. p. 281-306.

(34). Kaden DA, Call KM, Leong P-M, Komives EA, Thilly WG. Killing and mutation of human lymphoblast cells by aflatoxin B_1: Evidence for and inducible repair response. Cancer Res. 1987; 47:1993–2001. [PubMed: 3103909]

(35). Neal GE, Eaton DL, Judah DJ, Verma A. Metabolism and toxicity of aflatoxins M_1 and B_1 in human-derived in vitro systems. Toxicol. Appl. Pharmacol. 1998; 151:152–158. [PubMed: 9705898]

(36). Townsend AJ, Fields WR, Haynes RL, Doss AJ, Li Y, Doehmer J, Morrow CS. Chemoprotective functions of glutathione *S*-transferases in cell lines induced to express specific isozymes by stable transfection. Chem. Biol. Interact. 1998; 111:389–407. [PubMed: 9679569]

(37). Groopman J,D, Busby W,F Jr. Wogan GN. Nuclear distribution of aflatoxin B1 and its interaction with histones in rat liver in vivo. Cancer Res. 1980; 40:4343–4351. [PubMed: 7438068]

(38). Ozbal CC, Velic I, SooHoo CK, Skipper PL, Tannenbaum SR. Conservation of histone carcinogen adducts during replication: Implications for long term molecular dosimetry. Cancer Res. 1994; 54:5599–5601. [PubMed: 7923203]

(39). Roebuck BD. Hyperplasia, partial hepatectomy, and the carcinogenicity of aflatoxin B_1. J. Cell. Biochem. 2004; 91:243–249. [PubMed: 14743384]

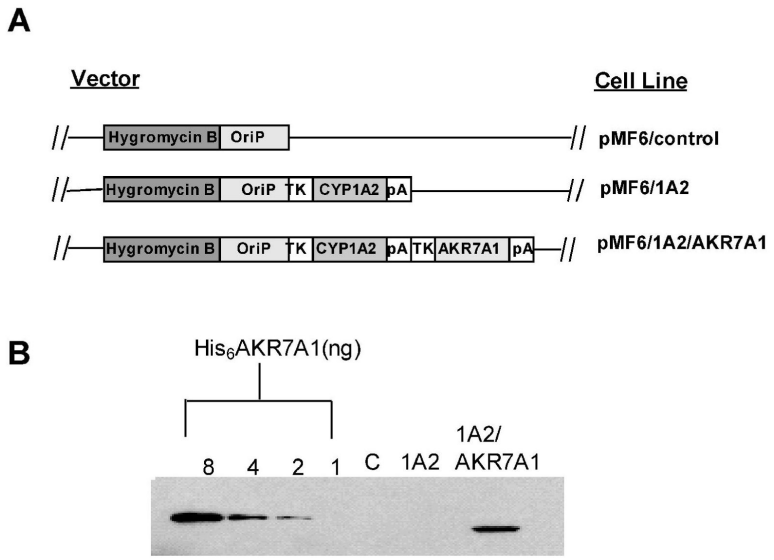

Figure 1.

(A) Diagram of the vectors used to construct the cell lines pMF6/control, vector control; pMF6/1A2, expressing human P4501A2; PMF6/1A2/AKR7A1, expressing human P4501A2 and rat AKR7A1. Key vector features include a resistance gene to hygromycin B, a cellular origin of replication (OriP), and thymidine kinase promoter (TK) and polyadenylation signal sequences (pA). (B) Immunoblot analysis of rat AKR7A1 in AHH-1 TK+/− cells. Cytosolic proteins (50 μg/lane) from transfected AHH-1 TK+/− cells were analyzed by immunoblot, using polyclonal rabbit anti-rat AKR7A1 raised against a bacterially expressed recombinant His_6-rat AKR7A1 protein. His_6-rat AKR7A1 protein was used as a standard for quantitation.

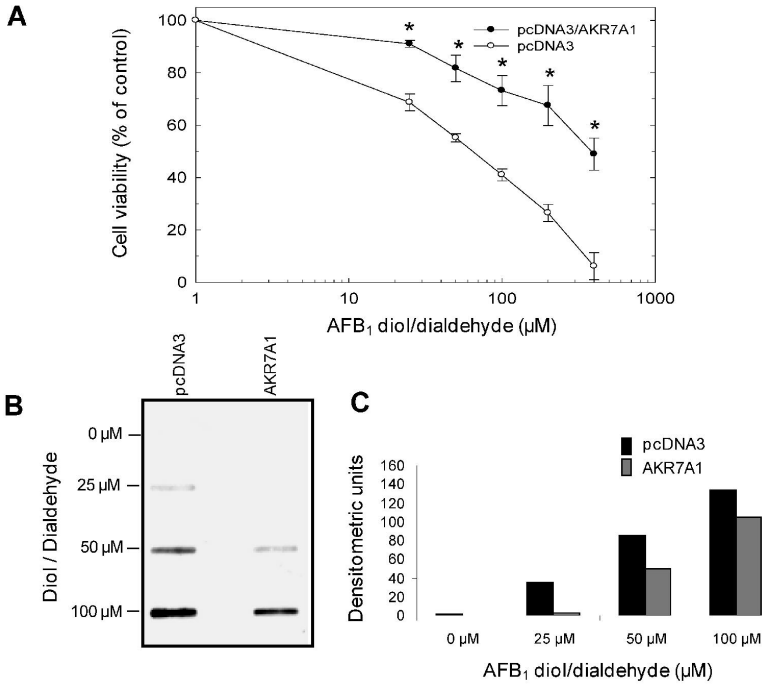

Figure 2.

(A) pcDNA3/control and pcDNA3/ AKR7A1 expressing COS-7 cells were treated with different concentrations of AFB_1 dialdehyde for 4 h, and cell viability was measured using the MTT assay. Error bars represent the means ± SE of three experiments repeated in triplicate (* indicates statistical significance in between cell viability at the same concentration, $p<0.05$). (B) COS-7 cells were transfected with pcDNA3/control and pcDNA3/AKR7A1 and challenged with serial concentrations of (0, 25, 50, 100 μM) AFB_1 dialdehyde. A qualitative assay for protein binding was devised using a slot-blot apparatus and an anti-lysine adduct primary antibody. (C) Densitometric analysis of protein adducts.

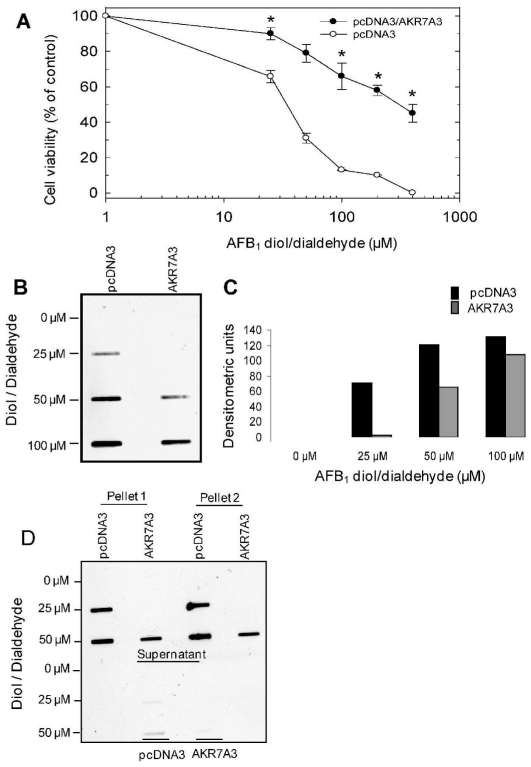

Figure 3.

(A) pcDNA3/control and pcDNA3/ AKR7A3 expressing COS-7 cells were treated with different concentrations of AFB_1 dialdehyde for 4 h, and cell viability was measured using the MTT assay. Error bars represent the means ± SE of three experiments repeated in triplicate (* indicates statistical significance in cell viability at the same concentration, $p<0.05$). (B) COS-7cells were transfected with pcDNA3/control and pcDNA3/AKR7A3 and challenged with serial concentrations of (0, 25, 50, 100 μM) AFB_1 dialdehyde. Protein adducts were detected using an anti-lysine adduct primary antibody. (C) Densitometric analysis of protein adducts. (D) Whole cell lysates from transfected COS-7 cells were fractionated and protein adducts detected as above.

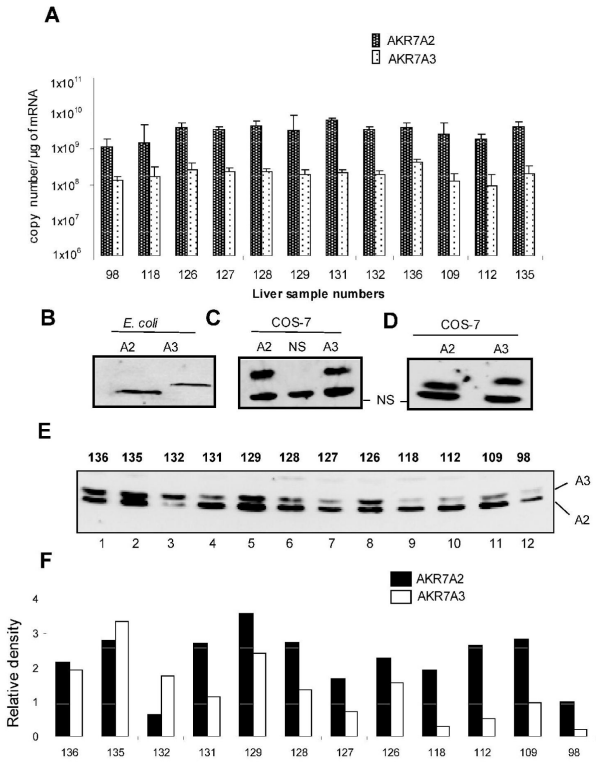

Figure 4.

(A) Real-time quantitative RT-PCR analysis of mRNA expression in 12 normal human liver tissues. AKR7A2 and AKR7A3 values were normalized to the level of β-actin in the same tissue. The results are shown as the means ± SD of three observations. (B). Western blot analysis of recombinant proteins of AKR7A2 and AKR7A3 were run on 4–15% gradient gel was probed with antisera against rat AKR7A1. (C) COS-7 cells transfected with AKR7A2 or AKR7A3 cDNAs expressed proteins were separated and immunoblotted as described in the Experimental Procedures. Untransfected COS-7 cells show a nonspecific band. (D) The same COS-7 expressed proteins were separated and immunoblotted on a gel containing a lower percentage of cross-linker as described in the Experimental Proceudres. (E) Detection of AKR7A1 immunoreactive protein(s) in human liver. Shown are human AKR7A2 and AKR7A3 representative immunoblots of cytosolic proteins samples prepared from twelve individual liver samples. (F) Presented are the results following densitometric analysis of the immunoreactive signals relative to sample 98, AKR7A2.

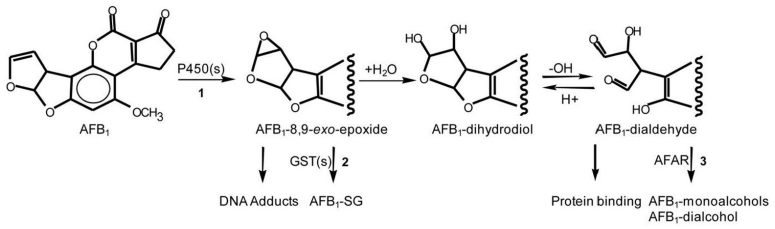

Scheme 1.

A schema of hepatic metabolism of AFB_1 depicting enzymatic and non-enzymatic fates of the AFB_1-8,9-*exo*-epoxide metabolite. Identified steps include **(1)** P450-catalyzed epoxidation of AFB_1 (P450-mediated biotransformation of AFB_1 also results in the production of polar hydroxylated metabolites, AFM_1, AFQ_1 and AFP_1); **(2)** GST catalyzed conjugation of the AFB_1-8,9-*exo*-epoxide with GSH; **(3)** AFAR catalyzed reduction of the AFB_1 derived dialdehyde.

Table 1

Binding of [^{3}H]AFB$_1$ to cellular DNA and cytotoxicity of AFB$_1$ in AHH-1 TK+/− cells

Cells were exposed to 3ng/mL [^{3}H]AFB$_1$ (15.8 Ci/mmol) or unlabeled AFB$_1$ for 28 hours. Cellular DNA was isolated as described in Experimental Procedures and binding measured by liquid scintillation counting. Values for DNA binding and relative survival are the result of one experiment performed with five replicate cultures of each cell line. Data is expressed as means ± standard deviation.

	AFB$_1$ binding to cellular DNA	
Cell line	**(fmol/mg DNA)**	**Relative Survival**
PMF6/control	1.3 ± 0.65	0.96 ± 0.06[b]
pMF6/1A2	284.0 ± 43.5[a]	0.73 ± 0.03
PMF6/1A2/AKR7A1	269.1 ± 11.9[a]	0.94 ± 0.09[b]

[a] DNA binding for pMF6/1A2 verses pMF6/1A2/AKR7A1 was not significantly different, P = 0.56.

[b] Relative survival is significantly different from pMF61A2, P < 0.005.